

In Vitro Deposition of Hydroxyapatite on Cortical Bone Collagen Stimulated by Deformation-Induced Piezoelectricity

Karem Noris-Suárez,^{*,†} Joaquin Lira-Olivares,[‡] Ana Marina Ferreira,[‡] José Luis Feijoo,[‡] Nery Suárez,[§] María C. Hernández,[§] and Esteban Barrios^{||}

Departamento de Biología Celular, Centro de Ingeniería de Superficies y Grupo de Polímeros del Departamento de Ciencias de los Materiales, and Departamento de Física, Universidad Simón Bolívar, Valle de Sartenejas, Aptdo 89000, Caracas 1081-A, Venezuela, and Laboratorio de Microscopía Electrónica, Departamento Tecnología de Materiales, I.U.T. Dr. F. Rivero Palacios, P.O. Box 350, San Antonio de Los Altos, Miranda 1204, Venezuela

Received August 25, 2006; Revised Manuscript Received December 2, 2006

In the present work, we have studied the effect of the piezoelectricity of elastically deformed cortical bone collagen on surface using a biomimetic approach. The mineralization process induced as a consequence of the piezoelectricity effect was evaluated using scanning electron microscopy (SEM), thermally stimulated depolarization current (TSDC), and differential scanning calorimetry (DSC). SEM micrographs showed that mineralization occurred predominantly over the compressed side of bone collagen, due to the effect of piezoelectricity, when the sample was immersed in the simulated body fluid (SBF) in a cell-free system. The TSDC method was used to examine the complex collagen dielectric response. The dielectric spectra of deformed and undeformed collagen samples with different hydration levels were compared and correlated with the mineralization process followed by SEM. The dielectric measurements showed that the mineralization induced significant changes in the dielectric spectra of the deformed sample. DSC and TSDC results demonstrated a reduction of the collagen glass transition as the mineralization process advanced. The combined use of SEM, TSDC, and DSC showed that, even without osteoblasts present, the piezoelectric dipoles produced by deformed collagen can produce the precipitation of hydroxyapatite by electrochemical means, without a catalytic converter as occurs in classical biomimetic deposition.

Introduction

The collagens are a large family of proteins defined by their ability to form highly organized supramolecular structures in the extracellular matrix of connective tissues, and by a common basic structural element of three parallel polypeptide α -chains folded into a triple helix.^{1,2} Collagen molecules consist of three α -chains, which wind around each other to form a thermally and proteolytically stable triple helix. Such a collagen triple helix shows a sharp transition to a random coil configuration close to body temperature, suggesting that minor changes of thermostability can be critical for the biological half-life of collagen.³ Collagen molecules are rod-like and are staggered one-quarter of their length from one another, forming microfilaments and filaments that pack laterally to produce macroscopically insoluble fibers.⁴ The range of denaturation temperatures of the solid-state collagen is an outcome of the degree of collagen cross-linking, water content, and the presence of substances like hydroxyapatite, and as a consequence the denaturation temperature range goes from 60 to near 250 °C.^{5,6} Among natural biopolymers, collagen deserves special attention. Its fundamental building block is believed to be the triple helical, dipolar tropocollagen unit, which aligns and stacks into fibril that exhibit an overall permanent dipole moment. The electrical-conduction properties of collagen are believed to result from this particular

alignment and close packing of the dipolar tropocollagen units, with the entire collagen fibril acquiring a permanent dipole moment.^{7,8} The triple-helical structure characterized by left-handed single chains with a right-handed twist and an overall permanent dipole allows a shielding effect of the surrounded thin water structures, which serves to maintain a situation of electron mobility in the physiological environment. In the *in vivo* tests, both parallel and antiparallel alignment of the dipolar tropocollagen units can be observed.⁸ However, *in vitro* collagen can exist only in the form of fibrils in which the dipolar tropocollagen units always align in the parallel state that results in a permanent dipole moment along the longitudinal molecular axis. It is possible to assume that sufficient disturbance to the native collagen structure, for example, an ionic imbalance and a change in water concentration, may affect the particular parallel alignment and condensed stacking of the molecule, with consequent changes in its electrical properties. These changes may in themselves be insufficient to give rise to extensive molecular rearrangement in the collagen, but sufficient to initiate a series of complex biochemical events with subsequent processes of adhesion and aggregation involving the collagen itself as well as the proteic substances with which it comes into contact.⁸

Some biological materials, like collagen and biopolymers, are found to exhibit the polar uniaxial orientation of molecular dipoles in their structure and can be considered as bioelectret. Such materials show piroelectricity and piezoelectricity.^{9,10} Collagen comprises 90% of the organic matrix in the bones and, together with the mineral (HA), governs the biomechanical properties and functional integrity of this tissue.¹¹

Bone collagen piezoelectricity and its influence on the physiology and functionality of bone have been highly

* Corresponding author. Tel.: +58 212 9064218. Fax: +58 212 9063064. E-mail: knoris@usb.ve.

[†] Departamento de Biología Celular, Universidad Simón Bolívar.

[‡] Departamento de Ciencias de los Materiales, Universidad Simón Bolívar.

[§] Departamento de Física, Universidad Simón Bolívar.

^{||} I.U.T. Dr. F. Rivero Palacios.

studied.^{12–16} However, the mineralization process has been so far accredited to the work of osteoblasts, which are attracted by the electrical dipoles produced either by piezoelectricity, due to deformation of the bone, especially the collagen in it, or due to outside electrical stimuli.¹⁷

Because collagen is constituted by polar repeating units of aminoacid ($-\text{CO}-\text{CR}-\text{NH}-$), the dielectric techniques are particularly sensitive to analysis by the relaxation phenomena in this material. In fact, these techniques have been used to study the effects of water on the dielectric properties of constituent phases of unmodified collagen.^{18–22}

The main purpose of this work was to study the mineralization process of cortical bone collagen induced by the effect of piezoelectricity in the material using a biomimetic approach in a cell-free system. The mineralization process was evaluated using scanning electron microscopy (SEM), thermally stimulated depolarization current (TSDC), and differential scanning calorimetry (DSC).

Experimental Section

Collagen Demineralization. Type I collagen was obtained from rabbits' bones and was demineralized as previously described.²³ Briefly, two femurs and tibias were demineralized by dissolving the mineral phase of the bone with a solution of EDTA 0.5 M, pH 7.4, under agitation at 4 °C, changing this solution for a fresh solution each 3 or 4 days. After 4 weeks, the samples were retired from the solution and washed thoroughly with distilled water to ensure that all EDTA was removed from the sample. To verify the degree of decalcification reached by the collagen, small samples of these were dyed with Alizarin-red;²⁴ this compound is sensitive to calcium and allows for verification of the presence of calcium in the materials or tissue. In the preparations, the amount of present calcium by means of this procedure was evaluated each week. After 4 weeks of decalcification, the amount of calcium present reached the lowest level of concentration attainable despite maintaining the samples for longer periods of treatment (3 months) with EDTA. The demineralized collagen obtained in this form is referred to subsequently as a control sample.

Deformation Process. The procedure used to deform the collagen substrates consists basically of bending the substrate inside a plastic tube, and maintaining it constrained, thus deformed, forming an arc co-incident with the internal radius of the tube that is 0.6 cm. This deformation assured a considerable stress, sufficient to elastically separate molecules of the collagen, thus generating the polarizing piezoelectric effect. The dipoles thus formed could induce the nucleation and deposition of the apatite. On the constraining tubes, relatively wide rectangular windows were opened, to provide direct contact of the sample with the simulated body fluid (SBF). Altogether, four collagen substrates were deformed and exposed to the SBF; a similar number of undeformed samples was used for calcification control. The samples were exposed for 4 weeks, on the average.

Biomimetic Tests. To simulate the blood plasma, a physiological fluid, following the specifications presented by Kokubo in the preparation of one simulated body fluid,²⁵ was prepared, thus using the so-called biomimetic method, to simulate the conditions for bone growth. SBF was prepared by dissolving reagent grade chemicals of NaCl, NaHCO_3 , KCl, $\text{K}_2\text{HPO}_4 \cdot 3\text{H}_2\text{O}$, $\text{MgCl}_2 \cdot 6\text{H}_2\text{O}$, CaCl_2 , and Na_2SO_4 into distilled water. It was buffered at pH 7.25 with 50 mM Tris-HCl. The fluid temperature was kept at 36.5 ± 0.5 °C and completely free from living cells or organic substances using sodium azide to inhibit microorganism growth. An acrylic column on a universal support was used, inside of which the substrates of collagen with and without deformation (that is, inside and outside constraining tubes) were submerged in the SBF. With the purpose of simulating the blood circulation in the body, an outside beaker that contained fresh SBF fluid was placed inside a stove to control the temperature to 37 °C,

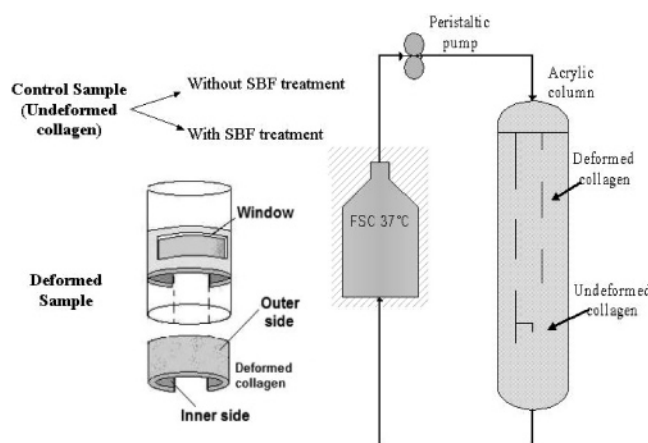


Figure 1. Schematic drawing of the experimental setup for the biomimetic system used for collagen mineralization.

and a peristaltic pump impelled the SBF to the column guaranteeing that it circulated cyclically throughout the column. The sample-containing column was thermally isolated to avoid heat exchange with the atmosphere, trying to maintain the temperature of the system nearest to body temperature. Figure 1 shows a schematic representation of the system. The solution of SBF was weekly replaced in the system by fresh solution. Also, the samples of deformed and undeformed bone cortical collagen were retired from the system weekly and preserved at -20 °C for analysis.

Scanning Electron Microscopy (SEM). The photomicrographs of the samples of collagen and collagen with hydroxyapatite (HA) deposits were obtained with a SEM, Phillips XL-30. Rectangular samples were prepared, lyophilized, and covered with a carbon layer. In addition, EDS (energy dispersion spectrophotometry) characterizations were made, yielding semiquantitatively the amount of calcium and phosphorus that had been deposited on the collagen substrate.

TSDC Analysis. In this study, the thermal stimulated depolarization current technique (TSDC) was employed to study the influence of the mineralization on the dielectric relaxation behavior of the collagen molecules. The TSDC technique is used to examine the variation with temperature of the depolarization current, produced by a sample that was previously polarized at a temperature T_p . The T_p should be sufficiently high to allow the orientation of the different dipolar species in the presence of an external electric field E_p . The technique is conducted at a low equivalent frequency ($\sim 10^{-3}$ Hz), allowing the accurate resolution of multicomponent peaks. By careful selection of the polarization conditions, it is possible to isolate a specific relaxation from a multitude of peaks. These characteristics make it possible to study the secondary relaxations (γ and β modes), as well as cooperative relaxations such as segmental (α mode) and higher temperature processes. The samples studied were rectangular shaped of approximately 0.40 cm^2 area and 600 micrometers thick. To avoid the effect of the conduction current and carrier injection on the depolarization spectra, the experiments were performed adding to both sides of the sample a pair of blocking electrodes. They were formed with a pair of sapphire disks of 19 mm in diameter and 0.216 mm thick. The sandwich was placed between two spring-loaded metallic electrodes in contact with the sapphire disks. The principle of the TSDC technique is based on the strong dependence of the dielectric relaxation time, τ , on temperature T . The state of polarization was frozen by quenching the sample rapidly (55 °C min^{-1}) to liquid nitrogen temperature. Next, the electric field was switched off, and the sample temperature was increased at a linear heating rate to record, with a Cary Vibrating Reed Electrometer model 401, the depolarization current caused by the disorientation of the dipoles. The sensitivity of our current measuring system was 10^{-17} A, and the signal-to-noise ratio was greater than 500. The constant heating rate used was 0.1 °C/s , and a typical electric field of $5 \times 10^5 \text{ V/m}$ was applied. Samples of different hydration levels had been studied by TSDC to follow the effects of water on the dielectric

properties of collagen. The hydration levels were varied by equilibrating the samples at room temperature in high vacuum (10^{-6} Torr). The hydration level, h (%), was calculated from the weight differences obtained at each step of the vacuum outgassing cycle. In all cases, the water content of the samples was determined from the loss of weight after drying to constant weight at 105 °C for 24 h. Hydration treatments were repeated in several samples to check reproducibility of the results obtained.

Differential Scanning Calorimetry (DSC). To determine the differences in thermal properties of the collagen and mineralized collagen samples, studies of differential scanning calorimetry (DSC) were employed using a Perkin-Elmer DSC-7; sample weights between 5.0 and 7.0 \pm 0.1 mg were used. The collagen samples were sealed in aluminum pans, under a nitrogen atmosphere of high purity. The range of temperatures studied went from 0 to 200 °C, and, when heated at the scanning rate of 20 °C/min, at least two replicas of collagen sample for each run were recorded. T_g measurements were determined using the midpoint inflection method. The temperature was controlled with a precision not less than ± 0.1 °C over the whole measured temperature interval. Samples with different levels of hydration were employed. Vacuum at room temperature during 44.17 h was used for dehydration of collagen.

Results and Discussion

Using the biomimetic system, represented schematically in Figure 1, the piezoelectric effect of the cortical bone collagen was evaluated with respect to the deposition of hydroxyapatite (HA) on the surface of the collagen material. For this purpose, a system was used that imitates the conditions of ion composition similar to the biological fluid, using the SBF²² with a pH and temperature at physiological conditions, and establishing a system of constant flow of liquid, to imitate *in vivo* conditions. In this study, the bone cells were excluded to study the piezoelectric effect of the collagen on HA precipitation.

To determine the influence of the collagen piezoelectricity originated by the mechanical deformation in the mineral deposition, the samples were immersed during a total period of 4 weeks as it was described previously. The undeformed (UNDS) and deformed (DS) samples were retired weekly for the corresponding analysis. The observations by SEM were made on the original two bone surfaces, that is to say, the internal face of the collagen surface, originally in contact with the endostium, and the external face, originally in contact with the periosteum.

The demineralized control sample was characterized by means of EDS with the purpose of measuring the amounts of Ca and P that were still present in both faces. From the micrographs of the surface, it is possible to observe the size and the amount of present crystals (Figure 2). A presence of dispersed white dots in the surface can be observed in the micrographs (Figure 2A and B). They could correspond to the HA from the original bone that was not dissolved during the process of bone demineralization. According to the EDS results, the amount of calcium and phosphorus is approximately between 1% and 3% of atoms on the substrate, which indicates that the initial decalcification generally occurred. However, these traces might be leftover from that initial demineralization process.

The DS and UNDS samples evaluated for the first and the second week of immersion in the SBF do not show an appreciable modification of the surface when compared to the control sample. The results of the percentage of Ca and P are small and comparable to the result obtained for the control sample.

The micrograph corresponding to the DS sample for the third week of immersion in SBF showed a higher mineral particle

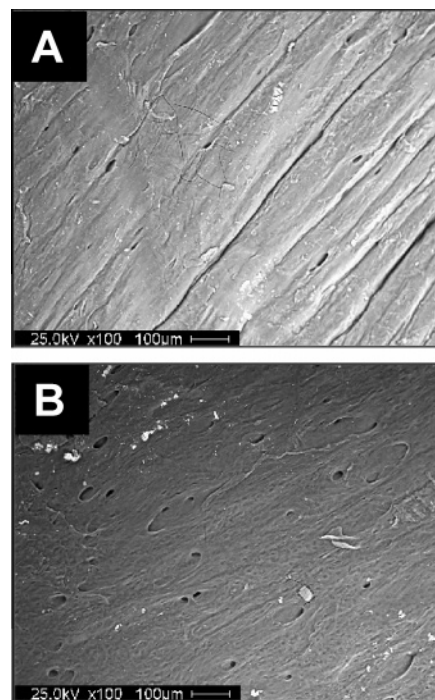


Figure 2. SEM micrographs of control sample bone cortical collagen (non-immersed in simulated body fluid). (A) Outer side (corresponds to periosteum bone surface). (B) Inner side (corresponds to endostium bone surface).

deposition on the compression zone (Figure 3B), as compared to the tension zone (Figure 3A). When making semiquantitative comparisons between the Ca/P relations in the compression zone to a magnification of 100 \times , the Ca/P relation obtained (Figure 3B) corresponds to 1.39 (see Table 1), which is very near the value of octacalcic phosphate (Ca/P is 1.33). Nevertheless, when the magnification is increased to 1000 \times (Figure 3C), the Ca/P relation obtained is 1.72, a value that is very near to the hydroxyapatite (Ca/P = 1.67). Comparing the results of EDS obtained for the DS substrates, it is possible to observe that the higher deposition occurs in the compression face.

The micrographs obtained by SEM for the samples immersed during 4 weeks in SBF are shown in Figure 3 (micrographs D–H). The micrographs of the UNDS sample immersed during 4 weeks are shown in Figure 3D and E. From this figure, it can be observed the presence of mineral deposits on both surfaces, although there was not a noticeable difference between the amount and the quality of these deposits when both faces are compared. Nevertheless, when the DS sample was immersed in SBF for 4 weeks, an important deposition formed on the surface subject to compression (Figure 3G) as compared to the surface under tension (Figure 3F). This preferential deposition is attributed to the piezoelectric effect generated by the application of a mechanical deformation in the collagen, causing the dipoles in collagen fibers to reorganize tending to increment of negative charges in the compression zone, favoring the nucleation and later the crystallization of the HA. The negative charges in the zone of compression apparently attract the calcium ions in solution that soon connect with the ion phosphate.¹² Increasing the magnification to 1000 \times , values near 1.69 were obtained for the atomic relation Ca/P of these particles (see Table 1); this value is close to the one of the hydroxyapatite stoichiometric proportion (Ca/P = 1.67) indicative that this is probably the mineral deposited in the zone of the cortical bone's collagen under compression. It should be emphasized that,

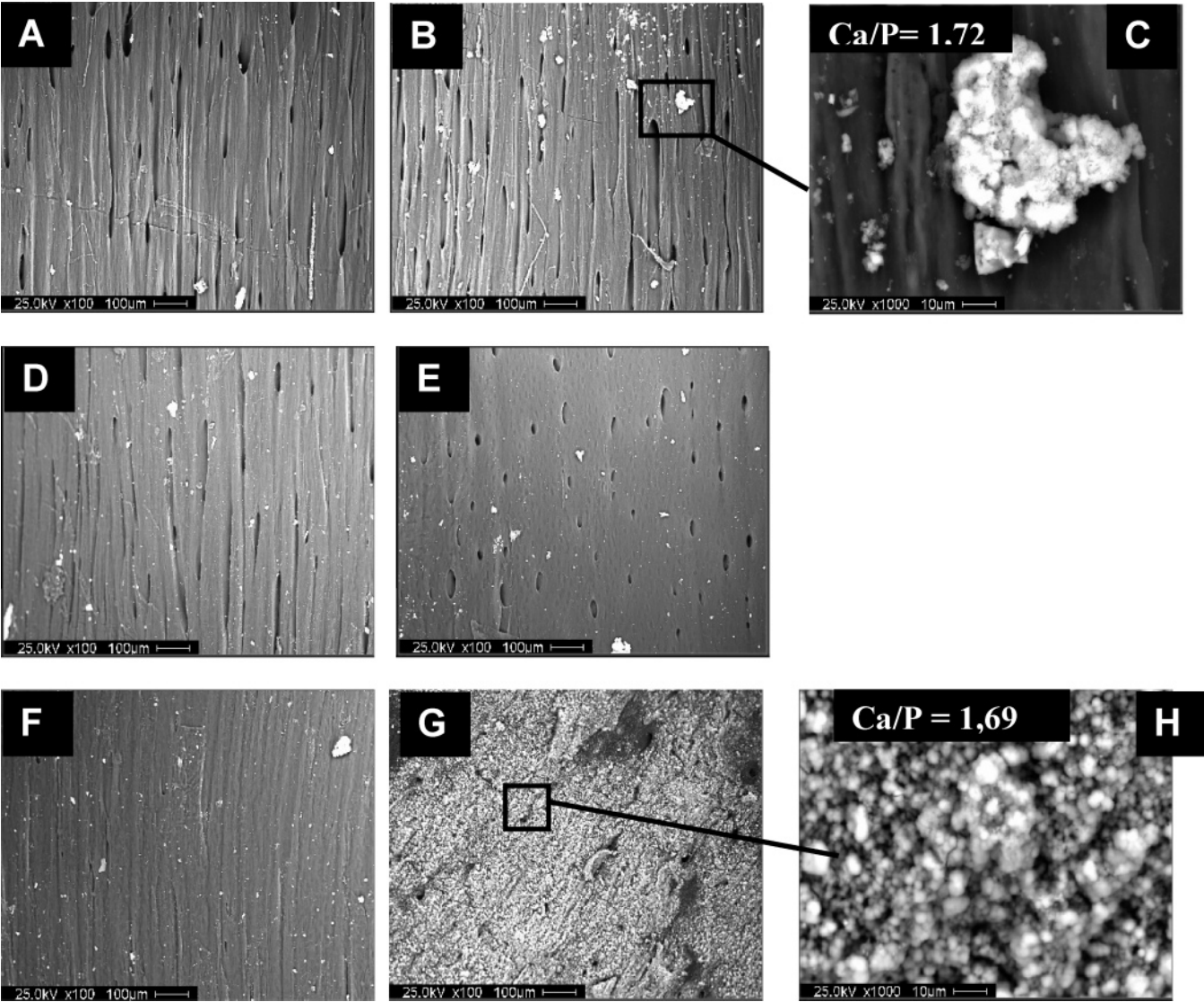


Figure 3. SEM micrograph of cortical bone collagen immersed in the simulated body fluid. (A) Tension deformed side after 3 weeks, (B) compression deformed side after 3 weeks, (C) detail of crystal observed on sample shown in micrograph B, (D) outer undeformed side after 4 weeks, (E) inner undeformed side after 4 weeks, (F) tension deformed side after 4 weeks, (G) compression deformed side after 4 weeks immersed, and (H) detail of compression deformed side after 4 weeks immersed.

Table 1. Ca and P Composition (%) and Ca/P Ratio of Cortical Bone Collagen, Analyzed by EDS

immersion time	collagen internal surface						collagen external surface					
	undeformed			deformed (compression)			undeformed			deformed (tension)		
	%Ca	%P	Ca/P	%Ca	%P	Ca/P	%Ca	%P	Ca/P	%Ca	%P	Ca/P
control	1.19	1.18	1.01	1.19	1.18	1.01	1.85	2.04	0.91	1.85	2.04	0.91
1 week 100×	0.62	0.61	1.02	1.46	1.84	0.79	0.85	0.81	1.05	1.46	1.84	0.79
3 weeks 100×	1.37	1.19	1.15	2.9	2.08	1.39	3.12	1.45	2.15	0.92	1.41	0.65
1000×				16.50	28.38	1.72						
4 weeks 100×	3.55	2.55	1.39	28.8	14.23	2.02	6.79	3.11	2.18	2.85	2.10	1.36
1000×				29.26	17.27	1.69				25.06	15.14	1.66

although the amounts of Ca and P present in the zone corresponding to endostium face (inner bone surface) in the 4 weeks immersed UNDS samples are very small when compared to those in the zone corresponding to the periostium face (outer bone surface), these values are bigger than those obtained for the control sample (see Table 1).

Studying the process of Ca deposition on collagen as a function of the immersion time in SBF (Table 1), it is possible to compare the immersed substrates in SBF with the control sample (not immersed), which have very little amount of

calcium atoms on their surface. All of the evaluated substrates DS and UNDS except the DS collagen external surface (tension side) showed an increase in the amount (%) of Ca and P atoms starting the third week; in particular, the increase in the zone of compression for DS samples was substantially higher when compared to the tension zone. In the case of DS collagen external surface, it is possible to observe that the amount of Ca and P atoms remains almost constant during the 4 weeks of immersion; these amounts are comparatively inferior to values found in the corresponding surface of the UNDS sample (6.79%

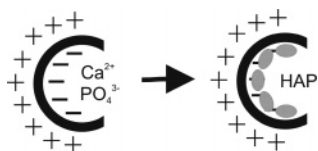


Figure 4. Schematic model of the biomineralization process.

Ca and 3.11% P) and comparable to the values found in the collagen external surface of the control sample.

For a long time, the growth of bone tissue has been described as a product of a mechanical stress. In 1982, Wolff systematized the study of this phenomenon, which nowadays is known as the Wolff Law.²⁶ In certain crystalline inorganic materials, which display an asymmetrical structure (lattice), the application of a mechanical stress results in the displacement of charges, generating the electrical dipoles, from surface to surface of the crystal. Diverse investigations confirm this phenomenon in the bone tissue.^{27–32} Studies made on the bone tissue demonstrated that, when applying a mechanical stress on the tissue, a negative polarity is created in all of the extension of the concave face (or compressed side), and a positive polarity is obtained in the convex surface of the bone (put under tension).^{12,26,28,29}

This difference of polarity on the faces of the bone tissue gave basis to the explanation of bone growth, due to negative polarity and the process of resorption on the side with positive polarity.^{12,33} In the experiments of deposition of HA that were carried out in the present work, using collagen cortical bone of rabbits and the biomimetic method, it was clearly observed that the preferential zone for the deposition of mineral is the zone under compression, when compared to the surface subject to tension. Figure 4 provides a model of the biomineralization process described above.

This suggests that the electrochemical action produced by generated piezoelectric dipoles can be the source of initial HA growth on the collagen substrate. Also, the depletion of HA from the side in tension, as compared to the immersed UNDS sample, could indicate that bone depletion could be also attributed, at least in part, only to electrochemical effects. If the deposition and depletion of HA were of electrochemical origin, this would suggest the application of electric fields to control bone molding.

Previous works made on bone molding aim at the biological phenomenon (osteoblast HA synthesis and osteoclast remotion), and the present work shows that the electrochemical phenomena produced by the piezoelectricity due to the deformation of the collagen added to that of the mineral bone determine the deposition and remotion of HA. The appearance of HA particles on the collagen is going to diminish its surface energy and contributes to create a new interface solid–fluid with a different dipole distribution. This new charge distribution could give a message to the osteoblasts to continue their tissue construction and the osteoclasts to remove HA from the opposite side. The cells probably participate in the bone molding stimulated either by the electrochemically deposited HA or by the piezoelectric polarization or by both. However, bone growth and molding could apparently occur by electrochemical effects only, without the activity of osteoblasts and osteoclasts.

Figure 5 shows the low-temperature dielectric spectra of three collagen samples: a demineralized bone collagen with no further treatment (control sample, week 0), a collagen sample 4 weeks immersed in the SBF solution (UNDS sample), and a collagen sample deformed (DS) and placed during 4 weeks in the SBF solution. TSDC experiments were performed in the following sequence: (a) the polarizing field was applied at room temper-

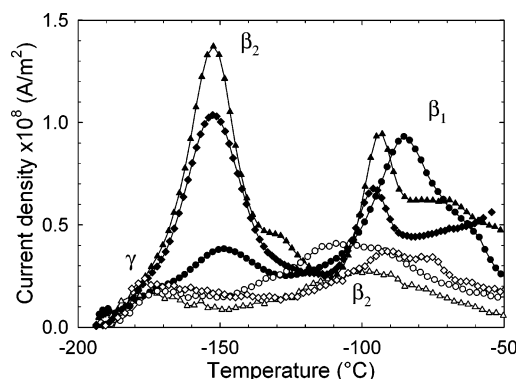


Figure 5. Low-temperature TSDC spectra of cortical bone collagen. The spectra correspond to two different hydration conditions: 10 min drying in high vacuum (first hydrated state, $h = 77\%$, filled symbols), and 20.17 h drying in high vacuum (second hydrated state, $h = 69\%$, open symbols). Δ = control sample (UNDS, week 0), \diamond = 4 weeks SBF immersed UNDS sample, and \circ = 4 weeks SBF immersed DS sample. The density current was normalized to an electric field of 1 MV/m. The intensity of the open symbol curves was magnified by 10. The polarization temperature of the spectra was 27 °C.

ature, after drying the samples in high vacuum during 10 min (first hydrated state with filled symbols in Figure 5); and (b) the same polarizing conditions but after further 20 h of high vacuum drying (second hydrated state with open symbols in Figure 5). The calculated hydration level of the three samples studied in the first and second hydrated state was 77% and 69%, respectively. The figure shows broad multicomponent relaxations with intensity variations among the different samples outgassed during 10 min. After 20 h of further outgassing, the three samples exhibit similar strongly attenuated spectra (there is a factor of 10 between the intensities), composed of a poor broad relaxation band located above -133 °C and a small shoulder around -173 °C. The remarkable spectra attenuation with outgassing time indicates that water plays an important role in the low-temperature relaxations of collagen. Nomura et al.³⁴ observed by mechanical measurements at 1 Hz two main modes on human dura matter collagen, labeled β_2 and β_1 , whose intensities increased, and they shifted toward lower temperatures with increasing water content. At above 25% water content, the temperature position of β_2 remains constant at -123 °C, while that of β_1 reaches the limited value of -73 °C above 50% water content. Maeda and Fukada³⁵ have also reported, on calcified and decalcified bones, by dielectric spectroscopy at 10 Hz, a peak at -110 °C that is shifted toward higher temperatures and diminished as the hydration level decreases. Fois et al.³⁶ studied, on human-bone collagen by TSDC, one main mode at -100 °C for a hydration of 10.5%. By analogy with these results, we believe that the TSDC mode observed in Figure 5 around -153 °C in the first hydrated state, and strongly attenuated and shifted toward higher temperatures in the second hydrated state, is the same mode labeled β_2 by Nomura et al.,³⁴ and the same dielectric relaxation as the ones reported by Maeda and Fukada³⁵ and Fois et al.³⁶ Table 2 resumes our results concerning the evolution with vacuum time of the temperature position of the mean relaxation peaks shown in Figure 5. The low-temperature position limit of the β_2 mode obtained in our experiments could account for the lower equivalent frequency of the TSDC experiments ($\sim 10^{-3}$ Hz) as compared to that corresponding in mechanical and dielectric measurements, and to the high water content of our samples in the first hydrated state (higher than 50% w/w). Concerning the origin of this relaxation, in accordance with these authors, it could be

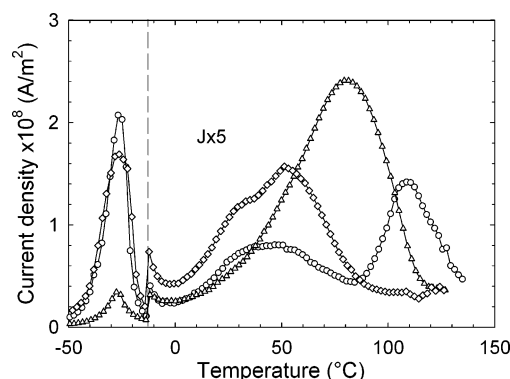
Table 2. Evolution with Vacuum Time of the Temperature Position of the β_2 and β_1 Peaks Shown in Figure 5

type of sample	vacuum time	T_m (°C)	
		β_2 peak	β_1 peak
control	10 min	-152.6	-93.9
	20.17 h	(-99, -97)	
4 weeks	10 min	-152.9	-95.4
	20.17 h	(-91, -88)	
UNDS	10 min	-149.2	-83.5
	20.17 h	(-111, -108)	

attributed to the relaxation of structural water, which is most strongly interacting with macromolecules.

In Figure 5, it is worth noting that at the first hydrated state, the maximum intensity ratio of the first to the second mean modes, β_2/β_1 , is about 1.4 for control sample (week 0) and 4 week immersed UNDS sample, while this ratio decreases to 0.4 for the 4 week DS sample. This observation coincides with the diminishing of the adsorption sites of water reported by Maeda and Fukada³⁵ in bone as compared to decalcified bone; therefore, it is an indication that β_2 process, that is, the relaxation of structural water, is being suppressed by the increasing amount of HA. As for the shoulder observed around -173 °C, it is stable in temperature for the three samples whatever the hydration level; therefore, by analogy with Nomura et al.³⁴ and Fois et al.,³⁶ this mode, labeled γ , could be attributed to the motion of aliphatic side chains. In Figure 5, the supplementary complex relaxation located in the temperature range from -93 to -53 °C cannot be distinguished after 20.17 h of vacuum outgassing. Similar water-dependent processes observed in wet skin collagenous tissue³⁷ and hydrated polypeptides³⁸ have been assigned to reorientation of loosely bound water molecules inserted into the material. Therefore, this mode, labeled as β_1 that can be easily erased after 20.17 h of vacuum outgassing, could be also attributed to motions of the hydrated side chains of glutamic acid, lysine, and other residues, which contain ionic side chains. The first hydrated state of the DS sample shows a shifting of the β_1 maximum toward higher temperature as compared to the same hydrated state of control and 4 week immersed UNDS samples. This effect can be thought of considering that this dielectric response depends upon the environment closed to the relaxing dipoles, and the apatite crystals located between the triple helixes and microfibrils must affect this surrounding.

Figure 6 shows the high-temperature spectra of the same collagen samples shown in Figure 4. The spectra were obtained after a total vacuum outgassing time of 44.17 h, and polarization at 127 °C during 3 min (third hydrated state). The calculated hydration level of the three samples studied in this hydrated state was 65%. The lower temperature zone was not included in these spectra as the weak and broad relaxation band shown in Figure 5 was masked by a huge relaxation, labeled T_{H_2O} , located at -28 °C. Similar findings have been reported by Nomura et al.³⁴ by mechanical measurements of collagen, and Bridelli et al.³⁹ by TSDC of hydrating biological macromolecules, and have been assigned to the melting of freezable water. Fois et al.³⁶ have also reported sharp peaks observed around ambient temperature and -6 °C, and by analogy with polyamides they conclude that these peaks should correspond to the break of hydrogen bonds between CO and NH in the amorphous phase, and between polypeptide chains and water molecules enclosed inside the triple helix. The similar temperature positions of the T_{H_2O} peak observed in Figure 6 and the relaxation reported by Nomura et al.³⁴ and Bridelli et al.³⁹ could allow the

**Figure 6.** High-temperature TSDC spectra of cortical bone collagen. The spectra were obtained after a total vacuum outgassing time of 44.17 h (third hydrated state, $h = 65\%$). Δ = control sample (UNDS, week 0), \diamond = 4 weeks SBF immersed UNDS sample, and \circ = 4 weeks SBF immersed DS sample. The density current was normalized to an electric field of 1 MV/m. The polarization temperature of the spectra was 127 °C.

assignment of this peak to the reorientation of melting freezable water. However, as this peak appears after polarizing the samples at 127 °C, and it is absent in the TSDC spectra of samples polarized at room temperature, further experimental evidence needs to be obtained to explain this peculiar behavior. The greater intensity of the T_{H_2O} peak for the samples placed in the SBF solution as compared to the control sample shows the influence of HA on this relaxation. Figure 6 also displays a higher temperature mode whose profile and temperature position vary with the HA content. The temperature position of this peak, labeled α peak, is located at 79.9 °C in the control sample. This temperature position is similar to the one reported by Fois et al.³⁶ for the glass transition of human collagen obtained by TSDC and DSC.

Consequently, the α peak shifting toward lower temperature observed in Figure 6 can be understood as dielectric evidence of the increasing mineralization process of the samples. The dielectric spectrum of the sample with the highest mineralization level showed also the split of the α mode into two modes, α_1 and α_2 located at 47.2 and 109.2 °C, respectively. This splitting, according to Samouillan et al.,⁴⁰ could be associated with some heterogeneity in the chain dynamics of collagen originated by the formation of different crystalline phases of apatite. The appearance of different crystalline phases at high mineralization levels could induce in some regions nearby the hardening of the polypeptide chains and thus slow their average segmental mobility. The TSDC results above-mentioned, especially those obtained for 4 week immersed DS collagen, show clearly that the interaction between the apatite crystals and the dipoles present in the collagen molecules is at the molecular level. Therefore, the α process is expected to be the dielectric manifestation of the collagen glass transition. According to the SEM micrograph of samples immersed in SBF solution, the mineralization process is initiated in the 4 week immersed UNDS sample and is enriched in the 4 week immersed DS sample.

Figure 7A shows the DSC thermograms of wet control sample, DS, and UNDS samples immersed 4 weeks in SBF; the three thermograms exhibit a large endothermic peak ranging from room temperature to 180 °C. This peak is ascribed to the heat of vaporization of adsorbed water;⁴¹ the differences in peak temperature and enthalpy of vaporization are mainly due to the different content in water in each sample, and it is not possible to relate these changes to the mineralization process. The shoulder located at around 65 °C on the thermograms of Figure

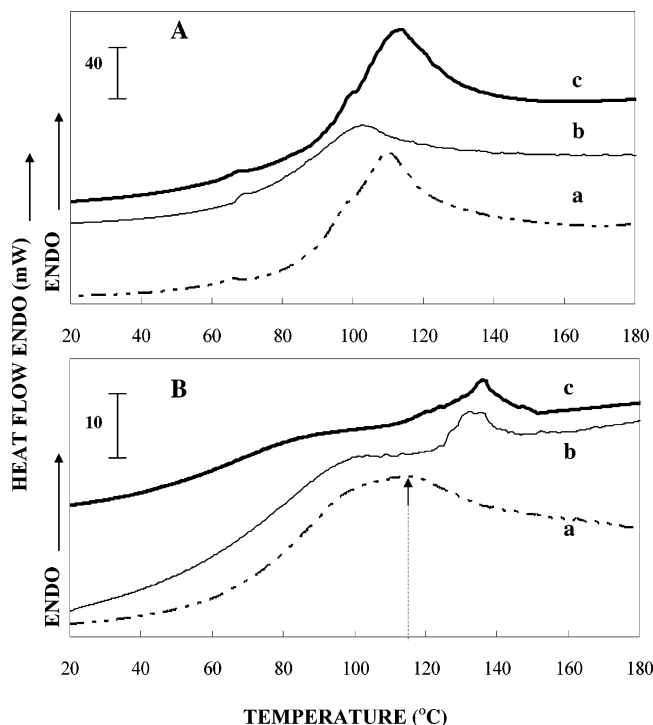


Figure 7. DSC thermograms of cortical bone collagen. (A) Hydrated samples: (a) control sample, (b) 4 weeks SBF immersed undeformed sample, and (c) 4 weeks SBF immersed deformed sample. (B) Thermograms of dehydrated samples outgassed in vacuum after a total of 44.17 h (third hydrated state, $h = 65\%$), and isothermally annealed at $127\text{ }^{\circ}\text{C}$ during 3 min: (a) control sample (arrow indicates T_d), (b) 4 weeks SBF immersed undeformed sample, and (c) 4 weeks SBF immersed deformed sample.

7A corresponds to the denaturation temperature (T_d) in collagen; this transition is masked by the large endothermic peak related to absorbed water. The lower value of T_d corresponds to the collagen reference sample.

Figure 7B shows the thermograms of dehydrated collagen samples outgassed in vacuum after a total of 44.17 h (third hydrated state, $h = 65\%$), and isothermally annealed at $127\text{ }^{\circ}\text{C}$ during 3 min, to simulate the condition for the TSDC samples of Figure 6. In this figure, the large endothermic peak is absent, and it is possible to observe a heat capacity step, demonstrating the existence of collagen glass transition in the range of $65\text{--}80\text{ }^{\circ}\text{C}$ for the three samples. The endothermic peaks occurring between 130 and $140\text{ }^{\circ}\text{C}$ on immersed UNDS and DS samples should correspond with the denaturation temperature; in these samples,⁴² the lower water content promotes the rising of T_d to a higher values if we compare to Figure 7A (hydrated samples). The deformed sample exhibits a higher T_d as a consequence of the HA mineralized on the sample when it is compared to the immersed non-deformed sample. In the case of the reference sample, the denaturation temperature is around $116\text{ }^{\circ}\text{C}$, which can be seen as a shoulder overlapping with the end of the T_g transition interval.

Table 3 shows a comparison between the temperature position of the α relaxation peak obtained by TSDC and the T_g values obtained using DSC. The temperature differences obtained for the same sample by the two techniques can account for the dissimilar heating rates used, being higher for DSC. The DSC T_g estimation of the dehydrated control sample presents a value that it is very close to the temperature position of the α relaxation peak obtained by TSDC for the same sample; this lower value obtained using DSC could be explained on the basis of a higher content of water in comparison with the control

Table 3. Comparison between the α Relaxation Temperature and the T_g Values Obtained Using DSC for Cortical Bone Collagen

bone collagen sample	T_g ($^{\circ}\text{C}$)	
	α peak ($\pm 0.2\text{ }^{\circ}\text{C}$)	DSC ($\pm 1.0\text{ }^{\circ}\text{C}$)
deformed (4 weeks SBF immersed)	47.2 ($\alpha_2 = 109.2$)	65
(4 weeks SBF immersed)	51.6	72
control (UNDS, week 0)	79.9	78–80

sample used for TSDC, as the control of water content during measurements is better achieved in the case of TSDC. The decreasing of these temperatures obtained by TSDC and DSC as the mineralization process proceeds is consistent with the findings shown in the SEM micrographs of Figure 3A–H. This result might be attributed to a decrease in the amount of hydrogen bonds as a result of the increased mineralization, resulting in an increase in the flexibility of collagen molecules having as a consequence the reduction of the T_g 's and the temperature position of the α relaxation peaks observed; these results are a consequence of the interaction between hydroxyapatite and collagen at the molecular level. The higher resolution of the TSDC method as compared to DSC allowed the observation of a second α mode (α_2), associated probably with the formation of different crystalline phases of HA, which is not possible to observe by DSC.

Conclusions

The effects of the mineralization process on DS and UNDS collagen samples were studied using SEM, TSDC, and DSC techniques. SEM results show that the mineralization effects were produced mainly in the bone collagen side deformed under compression, and this result suggests that the mineralization is produced by the piezoelectric effect induced in the sample immersed in the SBF. This implies that bone growth could apparently occur by electrochemical deposition only, without the activity of osteoblasts. Also, slight mineral depletion could occur without osteoclasts activity.

TSDC results show that the mineralization induces significant changes in the dielectric spectra of the compression-deformed sample. These changes could be observed at the localized low-temperature relaxations, as well as at the cooperative segmental modes. DSC and TSDC demonstrate the decreasing of the glass transition as the mineralization process proceeds. The sample with the highest mineralization level exhibits two α modes, probably associated with the formation of different crystalline phases of apatite. The changes observed in the dielectric relaxations with the evolution of the mineralization process revealed the TSDC technique as a very sensitive tool for the detection of the interaction between HA and collagen.

Finally, further studies are needed to understand better the role of piezoelectricity on the events that regulate the process of bone growth and remodelling.

Acknowledgment. We thank the Venezuelan National Science Foundation FONACIT through grants LAB-2000001639, G-200100900, and G-2005000449, and the Research and Development Unit (DID) of Simón Bolívar University (GID-02, GID-008, GID-35, CB-DID-014-05), for the support given to accomplish this work. We would like to thank the reviewers for carefully reading this manuscript. Their suggestions have indeed improved it. We acknowledge the sketch suggested by one of the referees depicting the process of mineralization on the surface of the deformed bone collagen.

References and Notes

- (1) Weiss, J. B.; Ayad, S. In ??; Weiss, J. B., Jayson, M. I. V., Eds.; Edinburgh: Churchill Livingstone, London, 1982; pp 1–27.
- (2) Burgeson, R. E. *Annu. Rev. Cell Biol.* **1988**, *4*, 551–577.
- (3) Notbohm, H.; Mosler, S.; Bodo, M.; Yang, C.; Lehmann, H.; Batge, B.; Muller, P. *J. Protein Chem.* **1992**, *11*, 635–642.
- (4) Ramachandran, G. N.; Chandrasekharan, R. *Biopolymers* **1968**, *6*, 1649.
- (5) Miles, C. A.; Avery, N. C.; Rodin, V. V.; Bailey, A. J. *J. Mol. Biol.* **2005**, *346*, 551–556.
- (6) Trebacz, H.; Wójtowicz, K. *Int. J. Biol. Macromol.* **2005**, *37*, 257–262.
- (7) Athenstaedt, H. *Ann. N.Y. Acad. Sci.* **1974**, *238*, 68.
- (8) Ravaglioli, A.; Krajewski, A. In *Bioceramics materials properties application*; Ravaglioli, A., Krajewski, A., Eds.; Chapman and Hall: London, 1991; pp 100–193.
- (9) Silva, C. C.; Thomazini, D.; Pinheiro, A. G.; Aranha, N.; Figueiro, S. D.; Goes, J. C.; Sombra, A. S. B. *Mater. Sci. Eng.* **2001**, *B86*, 210–218.
- (10) Kryszewski, M. *Acta Phys. Pol., A* **2004**, *105*, 389–408.
- (11) Knott, L.; Bailey, A. J. *Bone* **1998**, *22*, 181–187.
- (12) Marino, A. A.; Becker, R. O. *Nature* **1970**, *228*, 473–474.
- (13) Marino, A. A.; Becker, R. O. *Nature* **1975**, *228*, 627–628.
- (14) Nowick, A. S. *Nature* **1970**, *228*, 626–627.
- (15) Marino, A. A.; Becker, R. O.; Soderholm, S. C. *Calcif. Tissue Int.* **1971**, *8*, 177–180.
- (16) Hastings, G. W.; Mahmud, F. A. *J. Biomed. Eng.* **1988**, *10*, 515–521.
- (17) Young, R. W. *Clin. Orthop. Relat. Res.* **1966**, *45*, 153–156.
- (18) Samouillan, V.; Lamure, A.; Maurel, E.; Dandurand, J.; Lacabanne, C.; Ballarin, F.; Spina, M. *Med. Biol. Eng. Comput.* **2000**, *38*, 226–231.
- (19) Samouillan, V.; Lamure, A.; Lacabanne, C. *Chem. Phys.* **2000**, *225*, 259–271.
- (20) Marzec, E.; Warchol, W. *Bioelectrochemistry* **2005**, *65*, 89–94.
- (21) Freiss, W.; Lee, G. *Biomaterials* **1996**, *17*, 2289–2294.
- (22) Pietrucha, K.; Marzec, E. *Biophys. Chem.* **2005**, *118*, 51–56.
- (23) Noris-Suarez, K.; Romanello, M.; Bettica, P.; Moro, L. *Calcif. Tissue Int.* **1996**, *58*, 65–69.
- (24) Noris-Suarez, K.; Barrios de Arenas, I.; Vasquez, M.; Baron, Y.; Atias, I.; Bermúdez, J.; Morillo, C.; Olivares, Y.; Lira-Olivares, J. *Lat. Am. J. Met. Mater.* **2005**, *23*, 82–88.
- (25) Ebisawa, Y.; Kokubo, T.; Ohura, K.; Yamamuro, T. *J. Mater. Sci.: Mater. Med.* **1990**, *1*, 239–244.
- (26) Becker, R.; Marino, A. A. In *Electromagnetism and Life*; State University of New York Press: Albany, NY, 1982; pp 51–52.
- (27) Yasuda, I. *J. Jpn. Orthop. Surg. Soc.* **1954**, *28*, 267.
- (28) Fukada, E.; Yasuda, I. *J. Physiol. Soc. Jpn.* **1957**, *12*, 1198.
- (29) Bassett, C. A. L.; Becker, R. O. *Science* **1962**, *137*, 1063.
- (30) Becker, R. O.; Bassett, C. A. L.; Bachman, C. H. In *Bone Biodynamics*; Frost, H. M., Ed.; Little Brown: New York, 1964; pp 209–231.
- (31) Becker, R. O.; Brown, F. M. *Nature* **1965**, *206*, 1325.
- (32) Bassett, C. A. L.; Pawluk, R. J.; Becker, R. O. *Nature* **1964**, *204*, 652.
- (33) Marino, A. A.; Becker, R. O. *Clin. Orthop. Relat. Res.* **1974**, *100*, 247.
- (34) Nomura, S.; Hiltner, A.; Lando, J. B.; Baer, E. *Biopolymers* **1977**, *16*, 231–246.
- (35) Maeda, H.; Fukada, E. *Biopolymers* **1982**, *21*, 2055–2068.
- (36) Fois, M.; Lamure, A.; Fauran, M. J.; Lacabanne, C. *J. Polym. Sci., Part B: Polym. Phys.* **2000**, *38*, 987–992.
- (37) Mezghani, S.; Lamure, A.; Lacabanne, C. *J. Polym. Sci., Part B: Polym. Phys.* **1995**, *33*, 2413–2418.
- (38) Fenton, M.; Hiltner, H. *Biopolymers* **2004**, *17*, 2309–2314.
- (39) Bridelli, M. G.; Capelletti, R.; Vecchi, A. *J. Biochem. Biophys. Methods* **1992**, *24*, 135–146.
- (40) Samouillan, V.; Dandurand, J.; Lacabanne, C.; Hornebeck, W. *Biomacromolecules* **2002**, *3*, 531–537.
- (41) Okamoto, Y.; Saeki, K. *Colloid Polym. Sci.* **1963**, *194*, 124–135.
- (42) Kubisz, L.; Mielcarek, S. *J. Non-Cryst. Solids* **2005**, *351*, 2935–2939.

BM060828Z